Systems & Control Transactions

Original Research Article
Peer Reviewed Conference Proceeding
ESCAPE 36 - European Symposium on Computer Aided Process Engineering
Sheffield, UK. 21-24 June 2026

PSE PRESS

Towards Safety-Intelligent Cyber-Physical Systems: A Real-time Monitoring and Control Framework

Zhane Ann Tizon[abc], Yuanxing Liu[abc], Sahithi Srijana Akundi[abc], Austin Braniff[d], Beatriz Dantas[d], Yuhe Tian[d], Faisal I. Khan[bc], Efstratios N. Pistikopoulos[ab]*

[a] Texas A&M Energy Institute, Texas A&M University, College Station, TX, USA
[b] Artie McFerrin Department of Chemical Engineering, Texas A&M University, College Station, TX, USA
[c] Mary Kay O'Connor Process Safety Center (MKOPSC), Texas A&M University, College Station, TX, USA
[d] Department of Chemical and Biomedical Engineering, West Virginia University, Morgantown, WV, USA
* Corresponding Author: stratos@tamu.edu.

ABSTRACT

A safety-intelligent framework is presented for developing a multiple-input multiple-output (MIMO) risk-based explicit model predictive control (R-eMPC) for metal hydride storage systems (MHSS). These systems are susceptible to thermal runaway during the charging process as a result of the exothermic adsorption reaction within the metal alloy. To address this issue, deterministic and stochastic safety-intelligent control algorithms are designed and implemented by explicitly embedding a dynamic risk index (RI) or risk tolerance (α) into the control law and decision-making. In closed-loop analysis, the deterministic R-eMPC regulates both core temperature and hydrogen storage capacity by forecasting fault occurrence, triggering alarms, and reducing the risk index by adjusting the optimal control actions, supply pressure and water flowrate. Meanwhile, the stochastic R-eMPC accounts for uncertainties in core temperature variation by incorporating risk tolerance through chance-constraints. When the temperature exceeds the strict operational limit, stochastic R-eMPC enables continued operation beyond conservative safety boundaries via dynamic updated probabilistic limits. Closed-loop responses demonstrate that the safety-intelligent controllers effectively minimize evolving thermal risks while maximizing storage capacity during charging operation of the MHSS. Overall, the risk-based controllers improve both safety and charging performance, demonstrating the potential of the proposed framework for real-time, safety-intelligent operation of metal hydride systems.

Keywords: hydrogen, metal hydrides, model predictive control, process safety, multi-parametric programming, cyber-physical system

INTRODUCTION

Chemical and energy processes undergo different types of reactions, such as exothermic and endothermic reactions, during operation. When these reactions become uncontrollable, they can cause runaway incidents, leading to catastrophic damages such as fires or explosions, resulting in serious process safety issues [1]. Therefore, it is critical that reactive processes are properly monitored and controlled. However, most existing process control systems do not explicitly incorporate holistic safety metrics, instead treating safety through separate supervisory layers.

Hydrogen energy systems, encompassing production, storage, and utilization are inherently susceptible to hazardous events. Hydrogen storage represents a major safety bottleneck due to high energy density and reactive nature of hydrogen. Solid-state hydrogen storage using metal hydrides has attracted significant attention for fuel cell electric vehicles (FCEVs) because it can store hydrogen at relatively low pressures [2]. However, charging or adsorption process of metal hydride storage system (MHSS) is exothermic, where significant amount of heat is released, leading to rapid temperature rise. The reaction can be expressed in Eq. (1).

$$M + \frac{x}{2}H_2 \leftrightarrow MH_x + \Delta H \tag{1}$$

where M is metal alloy, H_2 is hydrogen gas, MH_x is metal hydride formation, and ΔH is heat of enthalpy.

In transportation application, the US Department of Energy (US DOE) specifies that the operating temperature of hydrogen storage should remain within between 233 K to 358 K [3]. Exceeding this temperature window may degrade system performance or compromise safety. Consequently, effective thermal management and control strategies are essential for MHSS.

Ali et al. [4] introduced a deterministic risk-based explicit MPC (R-eMPC) in which dynamic risk modeling as a function of a safety-critical variable was embedded in the control optimization. The R-eMPC was able to trigger the alarm system ahead of time to ensure enough time for the operators to shut down the system before any safety events occur. Akundi et al. [5] extended the safety-control theory by explicitly accounting for uncertainties by using Bayesian inference techniques and chance-constraints programming. In this study, the controller is allowed to be able to operate by exceeding the safety limit, thereby providing more flexibility in the presence of uncertainties. More recently, Liu et al. [6, 7] demonstrated the applicability of both online risk-based MPC and offline R-eMPC in a cyber-physical system of proton exchange membrane water electrolysis (PEMWE). The dynamic risk index was shown to effectively quantify evolving thermal risk and support real-time safety-aware operation.

Despite these advances, risk-based explicit MPCs have not yet been developed or validated for metal hydride hydrogen system (MHSS), where strongly exothermic reactions and strict thermal limits pose significant runaway risks. Hence, this study aims to develop a safety-intelligent control framework using deterministic and stochastic risk-based R-eMPC for MHSS, with particular emphasis on charging operation, while maintaining applicability to discharging operation and addressing the trade-offs between safety and performance.

METAL HYDRIDE STORAGE SYSTEM

This study focuses on metal hydride storage system (MHSS) to store hydrogen gas. Figure 1 demonstrates the schematic diagram of the charging process in MHSS with the metal hydride reactor, water tank, and process instrumentations. This analysis follows the schematic for modeling and simulation of the charging (adsorption) process, in which hydrogen gas is supplied from an external source, e.g. water electrolysis or refueling station. Since the reaction is exothermic and releases significant amount of heat, thermal management is incorporated through water supply is embedded in this system. Further, accurate modeling and real-time control implementation are crucial to ensure both safety and performance of the MHSS.

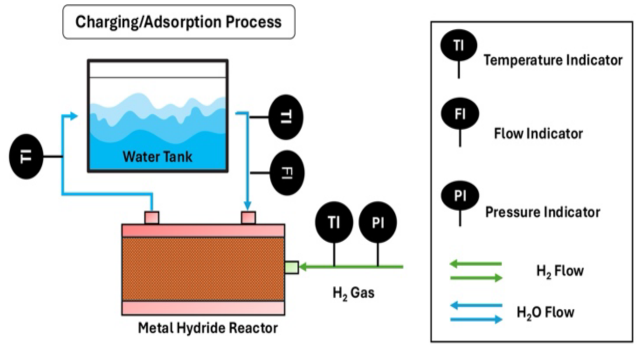

Figure 1. Schematic diagram of charging operation of metal hydride storage system.

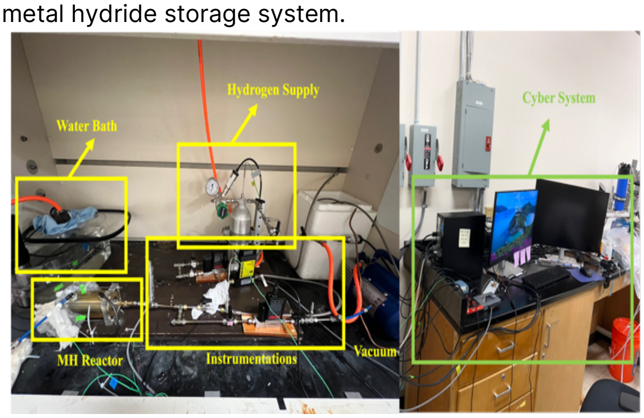

Figure 2. Experimental setup of metal hydride storage system.

High-Fidelity Model

The metal hydride storage model is developed using first-principles based on thermodynamics, reaction kinetics, and heat transfer mechanisms [8, 9, 10]. The governing equations are presented in Eqs. (2)-(10). These equations capture the coupled behavior of hydrogen uptake, reaction heat generation, and heat exchange between the metal hydride bed, reactor wall, and cooling medium.

$$\frac{dm_{H2,g}}{dt} = f_{in,H2} - rm_s \frac{MW_{H2}SC}{MW_{MH}} \tag{2}$$

$$m_{MH} = rm_{solid} \tag{3}$$

$$\left(m_{H2,g}C_{p,H2} + m_s C_{p,s}\right)\frac{dT_{MH}}{dt} = Q - \Delta H_a r_{ms} \frac{SC}{MW_{MH}} \tag{4}$$

$$r = C_a e^{-\frac{Ea}{RT}} \ln\left(\frac{Pa}{Peq}\right)\left(1 - \frac{m_{MH}}{m_s}\right) \tag{5}$$

$$P_{eq} = e^{\left(\frac{\Delta Ha}{RT} - \frac{\Delta Sa}{R} + 0.5\left(\pi\left(\frac{m_{MH}}{m_s} - 0.5\right)\right) + 0.1\right)} P_0 \tag{6}$$

$$m_{wall}C_{p,wall}\frac{dT_{wall}}{dt} = -h_{wall}A_{wall}(T_{wall} - T_{MH}) + Q \tag{7}$$

$$Q = f_{H2O}C_{p,H2O}\left(T_{H_2O,in} - T_{wall}\right) \tag{8}$$

$$\upsilon_j \rho_{H2O} C_{p,H2O} \frac{dT_{H2O,out}}{dt} = f_{H2O} C_{p,H2O} \left(T_{H_2O,in} - T_{H2O,out}\right) - Q \quad (9)$$

$$m_{H2,g} = \frac{PV_g}{RT} MW_{H2} \quad (10)$$

Cyber-Physical System

The experimental setup of the metal hydride storage system (MHSS) is illustrated in Figure 2. It consists of several integrated units, including a hydrogen supply (canister tank), metal hydride reactor, water bath, and associated process instrumentation. The system also incorporates a computer, data acquisition hardware, and a microcontroller to enable real-time data exchange and signal processing between the physical and cyber layers.

The cyber component primarily comprises the software and control algorithms used for monitoring, decision-making, and supervisory control. In this work, LabVIEW is employed for real-time data acquisition, signal conditioning, visualization, system identification, control implementation, and alarm monitoring. Measured process variables are continuously communicated to the control layer, where safety-intelligent control actions are computed and transmitted back to the physical system for real-time operation.

SAFETY-INTELLIGENT CYBER-PHYSICAL CONTROL ARCHITECTURE

For designing the safety-intelligent control strategies, this work adapts the PAROC framework [11] for both modeling and simulation and experimention. Figure 3 presents the framework on implementation of control strategies in cyber-physical system.

First, the system is modeled to capture its dynamic behavior under open-loop simulations. These simulations enable the a *priori* identification of potential safety events, such as thermal runaway, overpressurization, or fuel starvation, before conducting any physical experiments. The high-fidelity model is developed in Siemens Process Academics (Research). Subsequently, a cyber-physical system is developed by integrating both the experimental and cyber setups. The experimental component is designed based on a process and instrumentation diagram (P&ID) or a process flow diagram (PFD). The cyber component consists of a human–machine interface implemented using a customized LabVIEW platform, data acquisition for communication and data exchange, and a microcontroller for real-time control and operation.

Using the outputs and inputs of the open-loop data, a linear or surrogate model is derived using techniques such as system identification, model reduction, machine learning, or Jacobian-based linearization [12, 13, 14]. This linearized model then serves as the basis for designing safety-intelligent explicit model predictive control (MPC) strategies.

The formulations of deterministic and stochastic risk-based explicit MPC (R-eMPC) are presented in Eqs. (11)-(18) and Eqs. (19)-(26), respectively. The objective function aims to minimize the deviations in system outputs (y) from their corresponding setpoints, while simultaneously penalizing control efforts of the inputs (u). Eqs. (11) and (19) defines the weights for outputs and inputs matrices, QR and R, and output horizon (OH) and control horizon (CH), where k denotes the discrete timestep in seconds. The state-spaced models are given in Eqs. (12)-(13) and (20)-(21), where x represents state vector and A, B, C, and D are the system matrices. For the charging operation of the metal hydride, the outputs (y) correspond to the core temperature and hydrogen adsorbed capacity while inputs (u) are supply pressure and water flowrate.

Within the deterministic R-eMPC, dynamic risk assessment is conducted to compute a risk index, RI, which is defined as the product of event probability and severity as shown in Eq. (15). The resulting RI can be expressed as a function of safety-critical variable, enabling the controller to evaluate the safety level of the system during operation. Based on this assessment, R-eMPC mitigates risk propagation speed and severity, or raise the alarm when runaway reactions cannot be prevented during the operation.

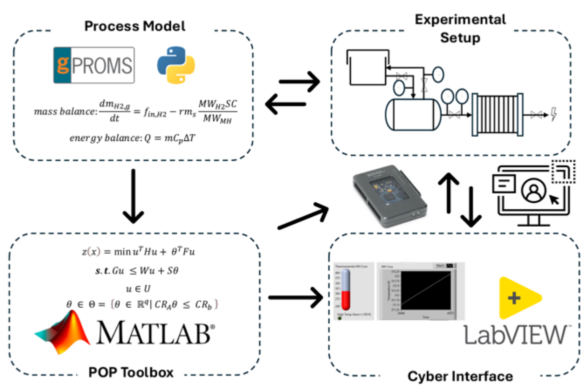

Figure 3. Safety-intelligent framework for cyber-physical systems.

$$min. J = \sum_{k=1}^{OH-1} QR\left(y_k - y_k^R\right)^2 + \sum_{k=1}^{CH-1} R\left(u_k - u_k^R\right)^2 \quad (11)$$

$$s.t.\, x_{k+1} = A_{xk} + B_{uk} \quad (12)$$

$$y_k = C_{xk} + D_{uk} \quad (13)$$

$$y_{min} \leq y \leq y_{max} \quad (14)$$

$$RI = P(y_{0,k}) \times S(y_{0,k}) \quad (15)$$

$$u_{min} \leq u \leq u_{max} \quad (16)$$

$$\Delta u_{min} \leq \Delta u \leq \Delta u_{max} \quad (17)$$

$$x_{min} \leq x \leq x_{max} \quad (18)$$

$$RI_{min} \leq RI(k) \leq RI_{max} \quad (19)$$

To account for the uncertainties during the operation of a system, stochastic R-eMPC (sR-eMPC) extends the deterministic R-eMPC through incorporation of risk tolerance (α) and chance-constraints within the optimization and decision-making framework. The design of sR-eMPC is based on Eqs. (20)-(27). The risk tolerance (α) can be calculated based on Bayesian inference in Eq. (22) to capture uncertainties of core temperature variations in metal hydride. As incorporated in Eq. (24), the chance-constraint update dynamic probabilistic limits to allow the system to operate beyond strict limits, thereby preventing unnecessary interventions or shutdown of the system. Further details on designing control optimization of the risk-based controllers can be found in Ali et al. and Akundi et al. [4, 5].

$$min. J = \sum_{k=1}^{OH-1} [QR(y_k - y_k^R)^2 + W(\alpha_k - \alpha_k^R)^2] + \sum_{k=1}^{CH-1} R(u_k - u_k^R)^2$$

$$s.t.\, x_{k+1} = A_{xk} + B_{uk} \quad (20)$$

$$y_k = C_{xk} + D_{uk} \quad (21)$$

$$P[Event|[y_k]] \leq \alpha_k \quad (22)$$

$$y_{min} \leq y_k \leq y_{max} \quad (23)$$

$$y_{0,k} - y_{0,threshold} \leq F^{-1}(\alpha_k) \quad (24)$$

$$u_{min} \leq u_k \leq u_{max} \quad (25)$$

$$\Delta u_{min} \leq \Delta u_k \leq \Delta u_{max} \quad (26)$$

$$x_{min} \leq x_k \leq x_{max} \quad (27)$$

The final step in this framework is to solve the risk-based control optimization via multi-parametric programming using POP Toolbox in MATLAB® [15]. This is an emerging technique to solve MPC explicitly, which means the optimization problem is solved once instead of iterating it every sampling time [16, 17]. Finally, during closed-loop implementation, the control actions is evaluated by computing the parameter vector, which includes hidden states, inputs, outputs, the risk index or risk tolerance, and setpoints. This parameter vector is then used to identify the feasible critical region, from which the appropriate control action is directly applied to the model or system. With the explicit R-eMPC solutions in place, the closed-loop performance of the system can be analyzed to demonstrate the effectiveness of both deterministic and stochastic risk-based control strategies.

RESULTS AND DISCUSSION

Open-loop Analysis

The dynamic behavior of the metal hydride storage system (MHSS) during charging is analyzed under open-loop conditions, without any control feedback. The charging or adsorption process involves supplying hydrogen gas to the metal hydride reactor, where H_2 is adsorbed within the lattices of the metal alloy, resulting in an exothermic reaction. A comparison between simulated and dynamically optimized responses of the core temperature and hydrogen adsorption capacity is presented.

For the open-loop simulation, the input variables, supply pressure and water flowrate, are set to prescribed values. In contrast, dynamic optimization aims to maximize the hydrogen adsorbed capacity while satisfying the operational constraints specified by the US DOE [3] within 300 seconds charging window.

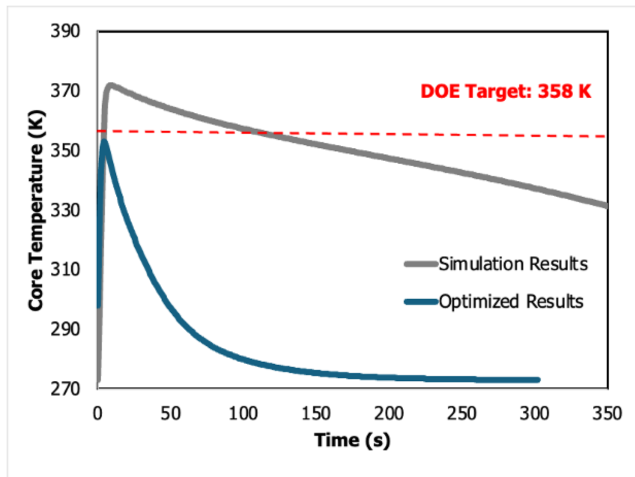

Figure 4. Core temperature trajectory during charging of metal hydride storage system during simulation and dynamic optimization.

Figure 4 compares the open-loop responses of core temperature obtained from simulation and optimization. In the simulated case, the supply pressure and water flowrate are set to 14 bar and 5 g/s, respectively. Under these conditions, the core temperature increases and reaches a peak of 378 K within 20 s, exceeding the recommended operating temperature limit of 358 K [3]. By comparison, the optimized response of core temperature peaks at 354 K, below the safety threshold, and achieves rapid cool down of the metal hydride. The optimal input profile determined by the optimization problem corresponds to a supply pressure of 14 bar and 12.46 g/s of water flowrate.

The corresponding hydrogen adsorbed capacity during open-loop simulation and dynamic optimization is shown in Figure 5. At a supply pressure of 14 bar and a water flow rate of 5 g/s, the simulated hydrogen storage capacity reaches only 0.9 wt.% within 300 s, indicating that the metal hydride does not reach saturation. In this case, the core temperature exceeds the thermal limit while the maximum storage capacity remains unattained. In contrast, the open-loop optimized response achieves a higher hydrogen storage capacity of 1.34 wt.% within the same time horizon. Therefore, these behaviors highlight a critical trade-off between faster charging rate and thermal safety, emphasizing the need for effective thermal management.

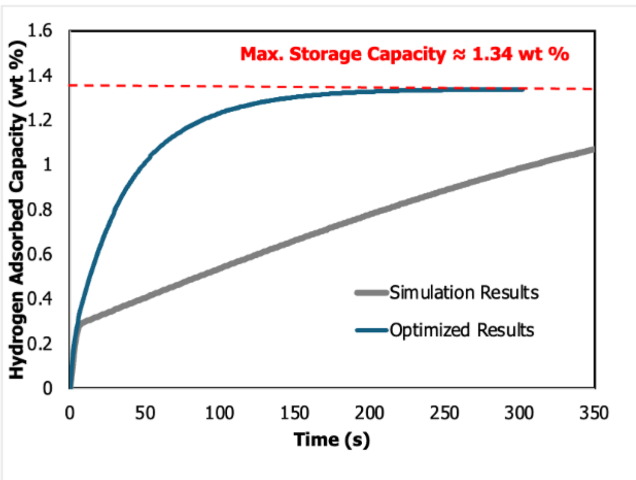

Figure 5. Hydrogen stored capacity trajectory during charging of metal hydride storage system during simulation and dynamic optimization.

The open-loop results demonstrate that while supply pressure improves charging efficiency and storage capacity, it also exacerbates thermal risks. These observations motivate the development of risk-based explicit model predictive control strategies to balance performance objectives with safety constraints under dynamic operating conditions.

Design of Risk-based Control Optimization

Deterministic and stochastic risk-based explicit control strategies were formulated based on the safety-intelligent control and optimization framework. The deterministic risk-based explicit MPC (R-eMPC) is designed according to Eqs. (11)-(18), where the core temperature is identified as the safety-critical variable due to the risk of thermal runaway during the charging process of the metal hydride storage system (MHSS). Figure 6 illustrates the dynamic risk analysis assuming a normal distribution of the core temperature, with a calculated mean (μ) of 290 K, a standard deviation (σ) of 11.35 K, and an upper control limit (μ + 3σ) of 324.05 K. Based on the analysis, the risk index limit is *RI* = 7.36, corresponding to the temperature limit = 358 K. Since the dynamic risk index is a temperature-dependent function that grows exponentially, a piecewise linear approximation is employed to obtain linear expressions suitable for embedding within the decision-making optimization problem.

Meanwhile, the stochastic R-eMPC (sR-eMPC), formulated in Eqs. (19)-(27), extends the deterministic framework by explicitly accounting for uncertainty through risk tolerance (α) based on Bayesian inference. In MHSS, the variation of core temperature is considered to analyze the risk tolerance during dynamic operation. In this formulation, α = 1 represents a fully safe operating condition, while α = 0 indicates a high-risk state. Compared to deterministic R-eMPC, the stochastic formulation provides additional operational flexibility by allowing controlled and temporary exceedance of temperature limits through chance-constraints. The chance-constraints incorporate the dynamically updated risk tolerance and are computed using inverse cumulative distribution function, as shown in Eq. (24), with a threshold temperature limit ($y_{0,\ threshold}$) of 358 K. Therefore, this allows the controller to satisfy the safety limits probabilistically, ensuring that constraints are met with a specified confidence level rather than deterministically.

Overall, the objective function of both safety-intelligent control strategies is to minimize excessive temperature peaks while maximizing hydrogen storage capacity within a finite time horizon during MHSS operation. Once the risk-based explicit MPC problem is solved using multi-parametric programming, explicit solutions to the optimization problem are obtained [15, 17]. These solutions are then implemented for closed-loop analysis of the metal hydride storage system.

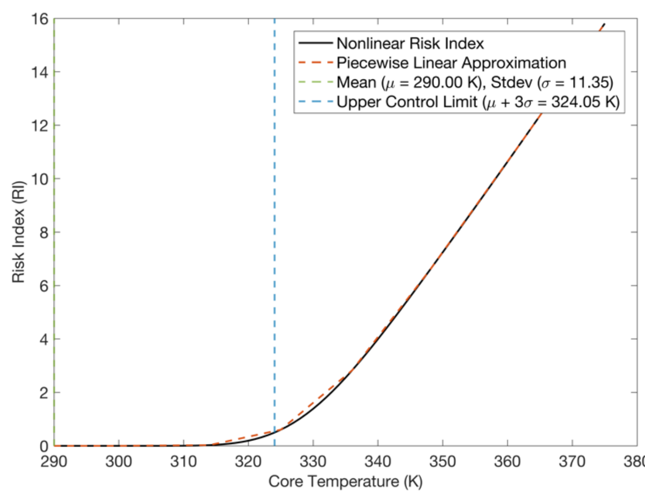

Figure 6. Dynamic risk analysis of core temperature during charging of metal hydride storage system.

Closed-loop Analysis

The resulting closed-loop responses are validated through simulation (*in-silico*) first using gO:MATLAB as the communication protocol between the system model in gPROMS and R-eMPC in MATLAB. The following subsection presents the analysis of both deterministic and stochastic R-eMPC strategies during charging operation of the metal hydride storage system.

Figure 7 presents the closed-loop responses of the metal hydride system under deterministic risk-based explicit MPC (R-eMPC) in *in-silico* simulations. The core temperature increases gradually and reaches a peak value of 372 K, exceeding the setpoint limit of 358 K. Simultaneously, the hydrogen storage capacity attains the maximum of 1.3 wt.% within 300 s. The risk index exhibits a trend similar to that of the core temperature and exceeds the specified risk limit when the temperature peaks. Although thermal runaway is not completely prevented, the controller effectively attenuates both the risk propagation rate and consequence severity.

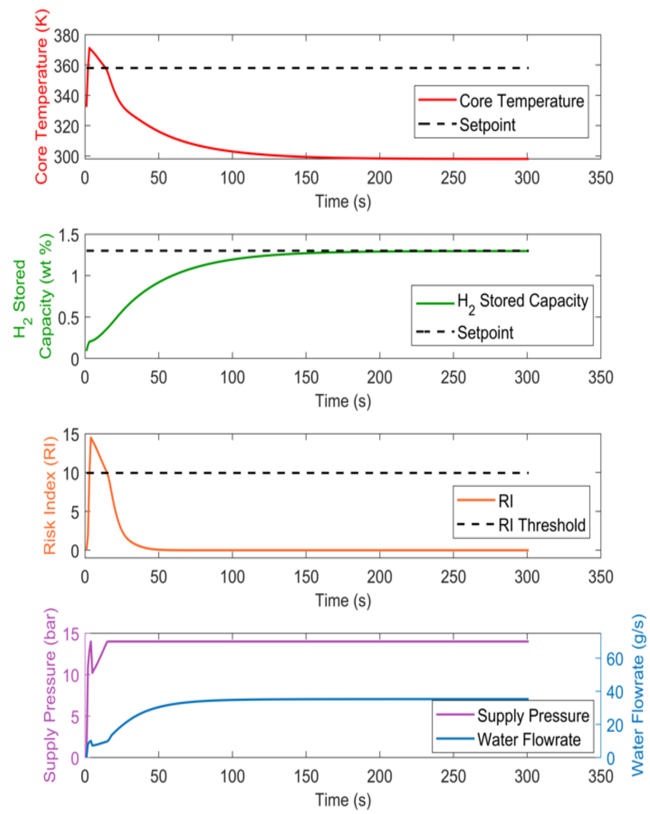

Figure 7. *In-silico* application of deterministic risk-based explicit MPC for closed-loop analysis of core temperature, hydrogen stored capacity, risk index and control actions.

At *t = 2 s*, the R-eMPC forecasts the risk index will exceed the limit in the next 10 seconds, which enable to trigger the alarm system ahead of fault occurrence time. While the risk index reaches a high value of *RI* = 14.5 at *t = 5 s*, the controller continues to act and successfully reduces both the risk and fault severity within 15 seconds. Here, the control actions are adjusted accordingly to manage the trade-offs between safety and performance. As a result, the R-eMPC effectively mitigates thermal risk while maximizing hydrogen storage capacity.

Figure 8 shows the in-silico performance of stochastic risk-based explicit MPC (sR-eMPC) during charging of metal hydride. The core temperature reaches a peak value of 367 K. Although this value exceeds the nominal temperature limit of 358 K, it remains below the maximum probabilistic limit of 371 K, demonstrating the increased operational flexibility of the stochastic controller and avoiding the need for a system shutdown.

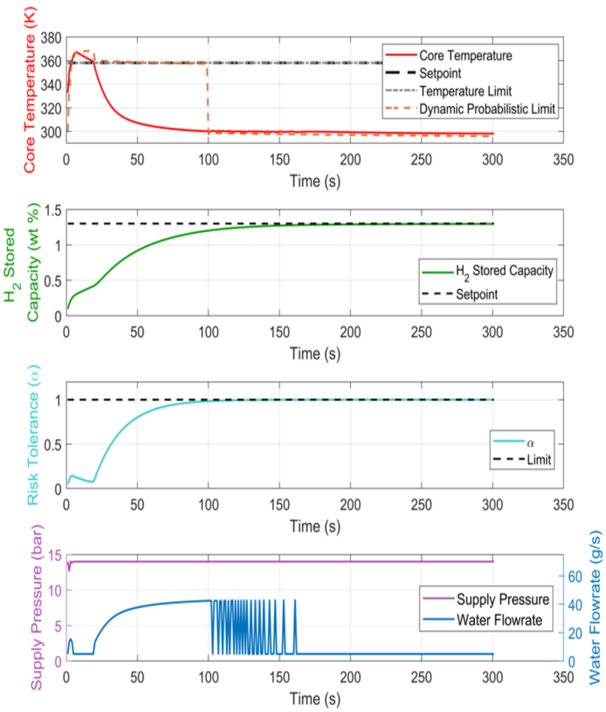

Figure 8. *In-silico* application of stochastic risk-based explicit MPC for closed-loop analysis of core temperature, hydrogen stored capacity, risk tolerance and control actions.

Unlike the risk index, the risk tolerance (α) evolves differently from the temperature profile. When it peaked at maximum, α = 0.1 indicating system is at state of risk. As adsorption process completes, the temperature gradually cools down and risk tolerance stabilizes to α =1. When the system operates in safe mode, the controller switches to predefined minimum control actions, corresponding to a supply pressure of 14 bar and a water flow rate of 5 g/s. At *t* = 170 s, the control system engages these predefined actions once the system is classified as safe according to the updated dynamic risk tolerance.

Moreover, the optimal control actions during closed-loop operation are provided by the controller to manage safety and performance. To achieve maximum storage capacity, the supply pressure maintains to be 14 bar. Meanwhile, as the temperature rises, the water flowrate increases to dissipate heat and maintain safe operation. As a result, sR-eMPC is able to allow the system to exceed the temperature limit and achieving full saturation within 300 s while satisfying the dynamic probabilistic limits.

CONCLUSION AND FUTURE WORK

This work presented dynamic modeling, experimental setup, control and operations of hydrogen storage using metal hydride in real-time. The safety-intelligent controllers, deterministic and stochastic R-eMPC, utilize risk indicators such as risk index and tolerance to assess safety level of the system and account for uncertainties, respectively. These were implemented to minimize the evolving thermal risks while maximizing the hydrogen capacity of metal hydride tank. Future work will include implementation of the stochastic risk-based explicit MPC into the cyber-physical setup of metal hydride storage for closed-loop analysis and validation.

ACKNOWLEDGEMENTS

The authors acknowledge financial support from NSF RETRO Project CBET- 2312457, Texas A&M Energy Institute, Mary Kay O'Connor Process Safety Centre (MKOPSC), and Department of Chemical and Biomedical Engineering at West Virginia University.

AUTHOR IDENTIFIERS

Author ORCIDs:
Tizon ZA: 0009-0006-9728-8224
Liu Y: 0000-0002-5895-8428
Akundi SS: 0000-0001-7711-7264
Braniff A: 0009-0006-6835-320X
Dantas B: 0009-0001-0446-7906
Tian Y: 0000-0001-7937-5785
Khan F: 0000-0002-5638-4299
Pistikopoulos EN: 0000-0001-6220-818X

REFERENCES

1. Saada R, Patel D, Saha B. Causes and consequences of thermal runaway incidents—will they ever be avoided?. Process Safety and Environmental Protection 97:109-115 (2015). https://doi.org/10.1016/j.psep.2015.02.005
2. Bellosta von Colbe J, Ares JR, Barale J, Baricco M, Buckley C, Capurso G, Gallandat N, Grant DM, Guzik MN, Jacob I, Jensen EH, Jensen T, Jepsen J, Klassen T, Lototskyy MV, Manickam K, Montone A, Puszkiel J, Sartori S, Sheppard DA, Stuart A, Walker G, Webb CJ, Yang H, Yartys V, Züttel A, Dornheim M. Application of hydrides in hydrogen storage and compression: achievements, outlook and perspectives. International Journal of Hydrogen Energy 44:7780-7808 (2019). https://doi.org/10.1016/j.ijhydene.2019.01.104
3. U.S. Department of Energy. Hydrogen Storage | Department of Energy n.d. https://www.energy.gov/eere/fuelcells/hydrogen-storage (accessed July 19, 2025).
4. Ali M, Cai X, Khan FI, Pistikopoulos EN, Tian Y. Dynamic risk-based process design and operational optimization via multi-parametric programming. Digital Chemical Engineering 7:100096 (2023). https://doi.org/10.1016/j.dche.2023.100096
5. Akundi SS, Liu Y, Braniff A, Dantas B, Shayan Niknezhad S, Tian Y, Khan F, Pistikopoulos EN. Towards intelligent safety-aware control systems – a stochastic risk-based explicit model predictive control strategy. Chemical Engineering Science 322:123052 (2026). https://doi.org/10.1016/j.ces.2025.123052
6. Liu Y, Akundi SS, Braniff A, Dantas B, Niknezhad SS, Tian Y, Khan F, Pistikopoulos EN. Process monitoring and safety?informed control of a proton exchange membrane water electrolysis system. AIChE Journal 71: (2025). https://doi.org/10.1002/aic.18909
7. Liu Y, Akundi SS, Tizon ZA, Braniff A, Dantas B, Tian Y, Niknezhad SS, Khan F, Pistikopoulos EN. Next?generation safety?aware cyber?physical system integration: a proton exchange membrane water electrolysis demonstration. AIChE Journal 72: (2026). https://doi.org/10.1002/aic.70211
8. Krokos CA, Nikolic D, Kikkinides ES, Georgiadis MC, Stubos AK. Modeling and optimization of multi-tubular metal hydride beds for efficient hydrogen storage. International Journal of Hydrogen Energy 34:9128-9140 (2009). https://doi.org/10.1016/j.ijhydene.2009.09.021
9. Talagañis BA, Meyer GO, Aguirre PA. Modeling and simulation of absorption–desorption cyclic processes for hydrogen storage-compression using metal hydrides. International Journal of Hydrogen Energy 36:13621-13631 (2011). https://doi.org/10.1016/j.ijhydene.2011.07.139
10. Aruna R, Jaya Christa ST. Modeling, system identification and design of fuzzy PID controller for discharge dynamics of metal hydride hydrogen storage bed. International Journal of Hydrogen Energy 45:4703-4719 (2020). https://doi.org/10.1016/j.ijhydene.2019.11.238
11. Pistikopoulos EN, Diangelakis NA, Oberdieck R, Papathanasiou MM, Nascu I, Sun M. Paroc—an integrated framework and software platform for the optimisation and advanced model-based control of process systems. Chemical Engineering

Science 136:115-138 (2015). https://doi.org/10.1016/j.ces.2015.02.030
12. Kravaris C, Kookos IK. Understanding process dynamics and control. Cambridge University Press (2021). https://doi.org/10.1017/9781139565080
13. Wang W, Wang Y, Tian Y, Wu Z. Explicit machine learning-based model predictive control of nonlinear processes via multi-parametric programming. Computers & Chemical Engineering 186:108689 (2024). https://doi.org/10.1016/j.compchemeng.2024.108689
14. Dantas B, Braniff A, Liu Y, Akundi SS, Tizon ZA, Niknezhad SS, Khan F, Pistikopoulos EN, Lima FV, Tian Y. Hybrid mechanistic/data-driven modeling for enhancing dynamic operations in electrolysis-based hydrogen production. International Journal of Hydrogen Energy 207:153544 (2026). https://doi.org/10.1016/j.ijhydene.2026.153544
15. Oberdieck R, Diangelakis NA, Papathanasiou MM, Nascu I, Pistikopoulos EN. POP - Parametric Optimization Toolbox. Ind Eng Chem Res 2016;55:8979–91. https://doi.org/10.1021/ACS.IECR.6B01913/ASSET/IMAGES/LARGE/IE-2016-01913A_0011.JPEG
16. Tøndel P, Johansen TA, Bemporad A. An algorithm for multi-parametric quadratic programming and explicit MPC solutions. Automatica 39:489-497 (2003). https://doi.org/10.1016/s0005-1098(02)00250-9
17. Pistikopoulos EN. Multi?parametric optimization and control. Wiley (2020). https://doi.org/10.1002/9781119265245